Design, fabrication and characterization of a ultra-high-Q resilient Nb_3Sn resonant cavity

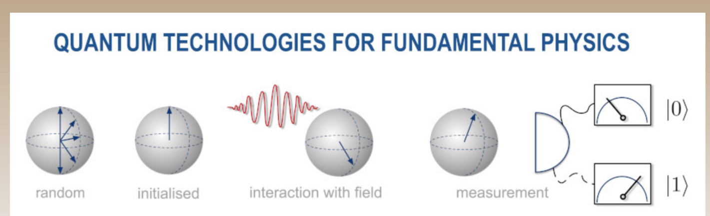

Alessio Rettaroli (alessio.rettaroli@lnf.infn.it)
INFN – LNF, Frascati (Rome), Italy

1. Axions and the LNF haloscope

- One open question of fundamental physics is what is dark matter made of. One possible candidate is the axion, a particle initially introduced in a Beyond-the-Standard-Model theory to solve the strong CP problem. It can be abundantly produced in the early Universe with a non-thermal process and may constitute the dark matter halo of our Galaxy. From the interaction Lagrangian, the conversion of an axion into a photon when subject to a strong magnetic field is predicted. In order to search for axions, haloscopes are required: they are constituted of resonant cavities in high magnetic fields, to stimulate the conversion of axions into photons. All the setup is kept at cryogenic temperatures with a dilution refrigerator, and the signal is amplified by ultra-low-noise receivers. The signal power is proportional to:

$$P_{a\gamma} \propto g_{a\gamma}^2 V Q B^2,$$

where $g_{a\gamma}^2$ is the coupling constant to the photons, V and Q are the volume and the quality factor of the resonant cavity, whereas the scan rate and the signal-to-noise ratio both depend also on the noise temperature T_n of the system.

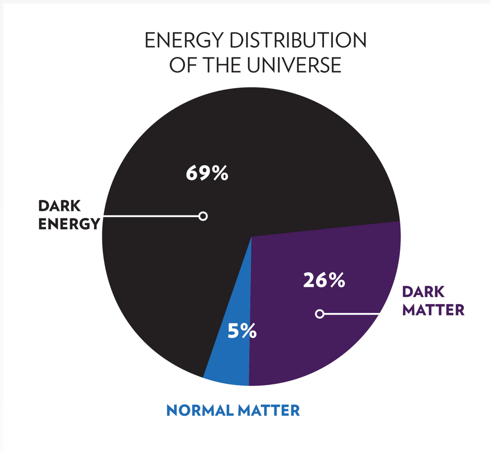

$$\mathscr{L}_{a\gamma\gamma} = -g_{a\gamma\gamma} a \vec{E} \cdot \vec{B}$$

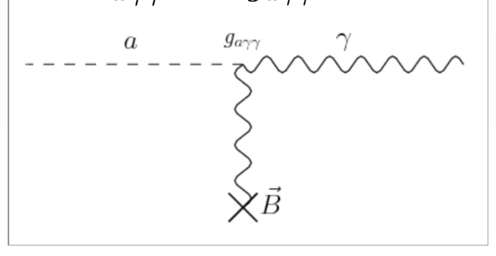

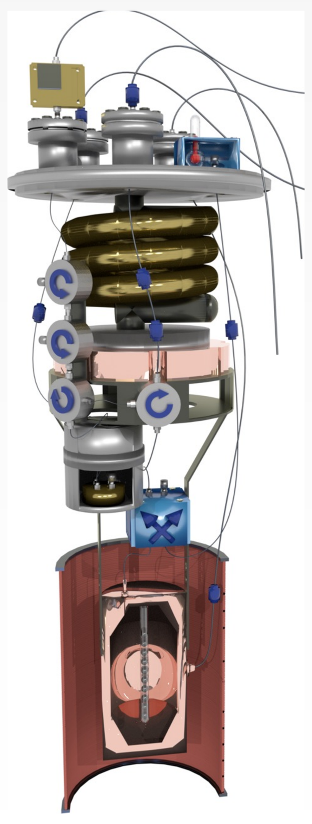

- Many avenues to push further the haloscope sensitivity are being tested at LNF, facing some technological challenges. One of these is the development of **superconducting cavities**, which show a higher quality factor Q with respect to copper. Additionally, the superconducting material has to be sufficiently resilient to the applied static magnetic field. The LNF haloscope is constituted of a dilution refrigerator able to reach 10 mK of base temperature in which a resonant cavity of order some centimeters of diameter is put in the bore of a SC magnet providing up to 9 T magnetic field. As a low-noise preamp stage, the haloscope will be soon provided with a JPA or TWJPA.

Besides the SC cavities research, the LNF labs are also committed to develop quantum sensing devices, such as a microwave single photon counter based on the switching of a **Josephson junction**, or a **qubit** technology.

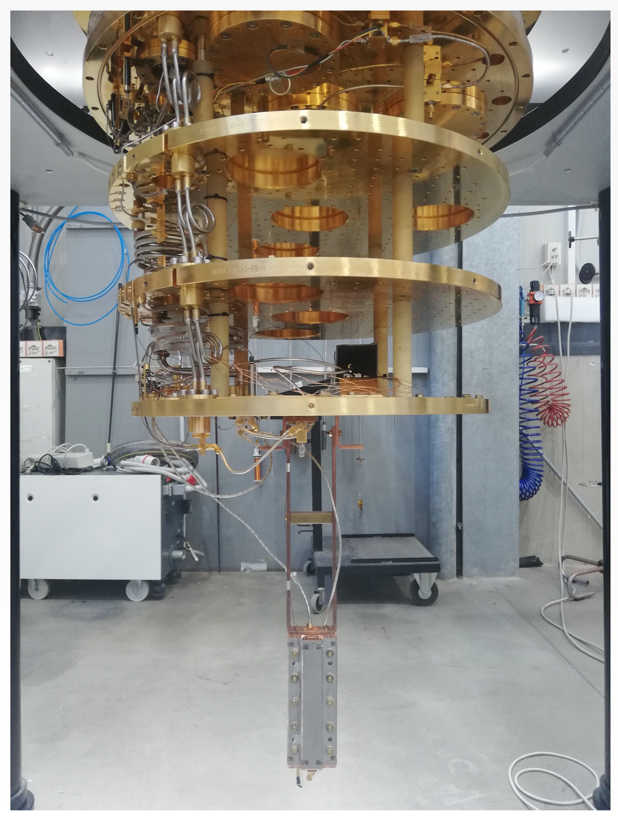

2. Fabrication of Nb_3Sn superconducting cavity

The cavity was designed at **LNF** and **FNAL** to optimize the coupling of axions with photons; this requires the use of the TM010 mode. The frequency is about 9 GHz, and this corresponds to an axion mass of about 37 μeV. The cavity is designed with a cigar shape so that the dissipative losses of the rf currents are

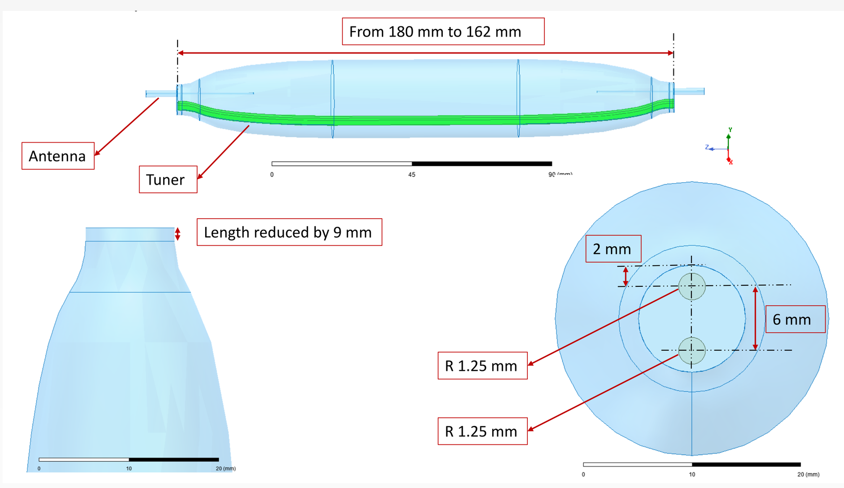

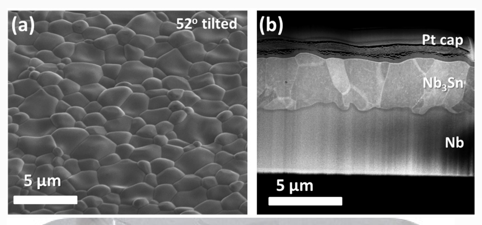

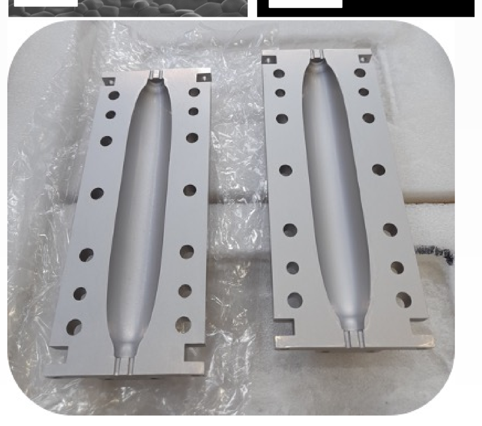

negligible in the endcaps, because of the cut-off region created therein. The possibility to have a tuning rod to scan different axion masses has also been studied.

The fabrication process starts hollowing a piece of bulk niobium (Nb), which as a SC has a critical temperature of 9 K. Then, after electropolishing of the Nb, the cavity has been coated with tin (Sn) with a vapour diffusion technique. The temperature of the furnace has to be > 950 °C, at which temperature the low-T_c phases of Nb–Sn (Nb_6Sn_5 and $NbSn_2$) are thermodynamically unfavorable and the Nb_3Sn stechiometry is naturally favored. Finally, the cavity is rinsed with high pressure ultra-pure water, and assembled in a class 10 cleanroom. The resulting film of Nb_3Sn over the Nb substrate is about 2–3 μm, and the expected critical temperature and critical field are of 18 K and 30 T.

3. Simulations

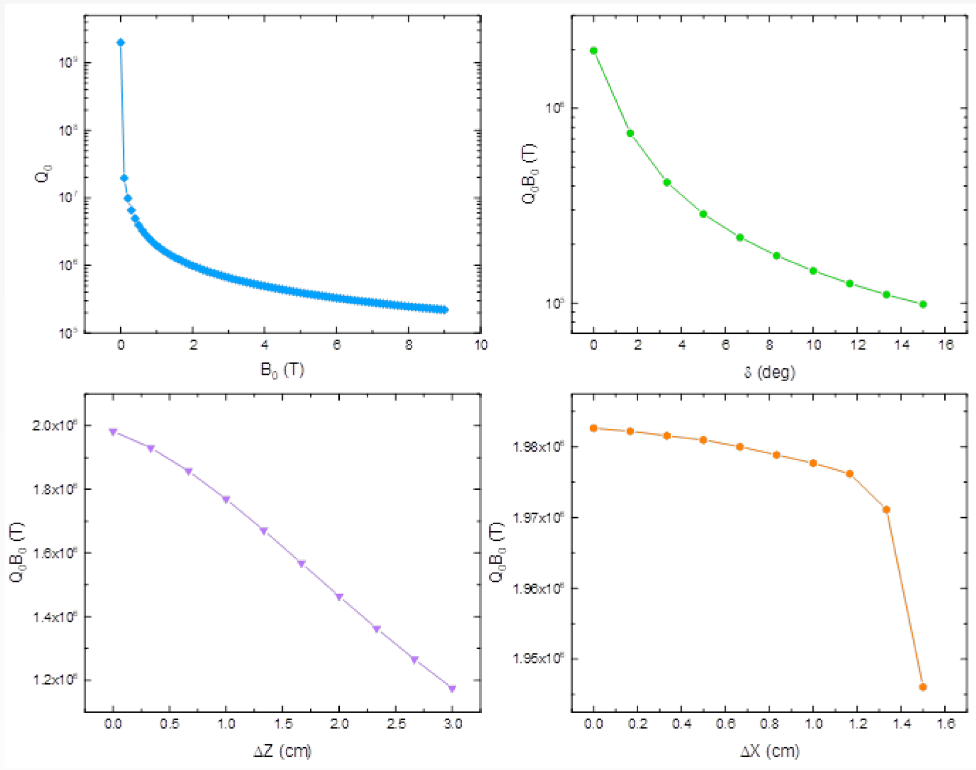

In a SC, the London depth λ can be a rough substitute of the skin depth δ in the estimation of the R_s. From the simulations, $G \simeq 450\ \Omega$, while the values of λ and R_s are found in literature, $\lambda \approx 160$ nm and $R_s = 50\ \mathrm{n}\Omega \div 50\ \mu\Omega$ from 0 T to 9 T.

The main result of the simulation shows the Q_0-vs-B dependence. The quality factor at 0 T is $\mathbf{2 \times 10^9}$, and after a rapid exponential decay, the Q_0 reaches almost a constant value at 9 T, which is $\mathbf{2.5 \times 10^5}$. The other plots show the degradation of the $Q_0 B$ product with various misalignments of the cavity in the magnetic field. Of particular interest is the tilt of the cavity axis with respect to the magnetic field axis (green plot).

To simulate the dependence of the quality factor with the magnetic field it is necessary to solve Maxwell's equations. This has been done with COSMOL by the group at FNAL, and with ANSYS-HFSS by the group at LNF. The 3D plots of the resonant modes are visible in the bottom figure, while the Q_0-vs-B dependence is shown in the upper left plot. The mode of interest is the TM010. The Q_0 can be expressed as

$$Q_0 = G/R_s, \qquad R_s \simeq 1/\lambda\sigma$$

where G is a geometrical factor and R_s the surface resistance.

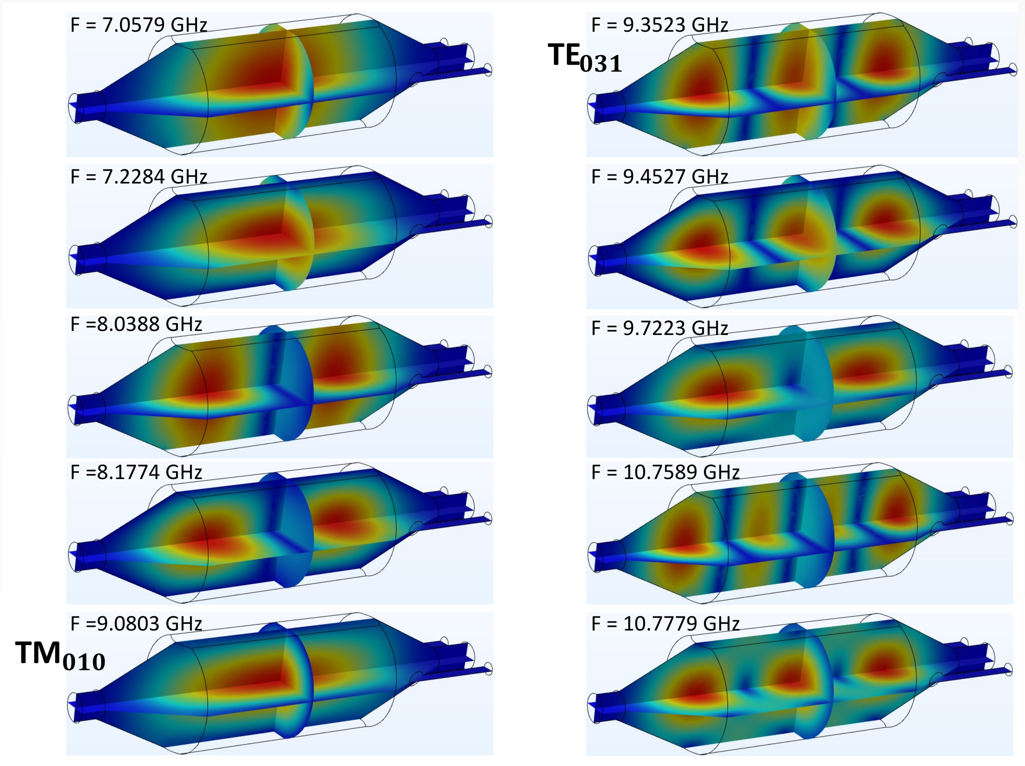

4. Q_0 vs B Characterization at LNF and axion search

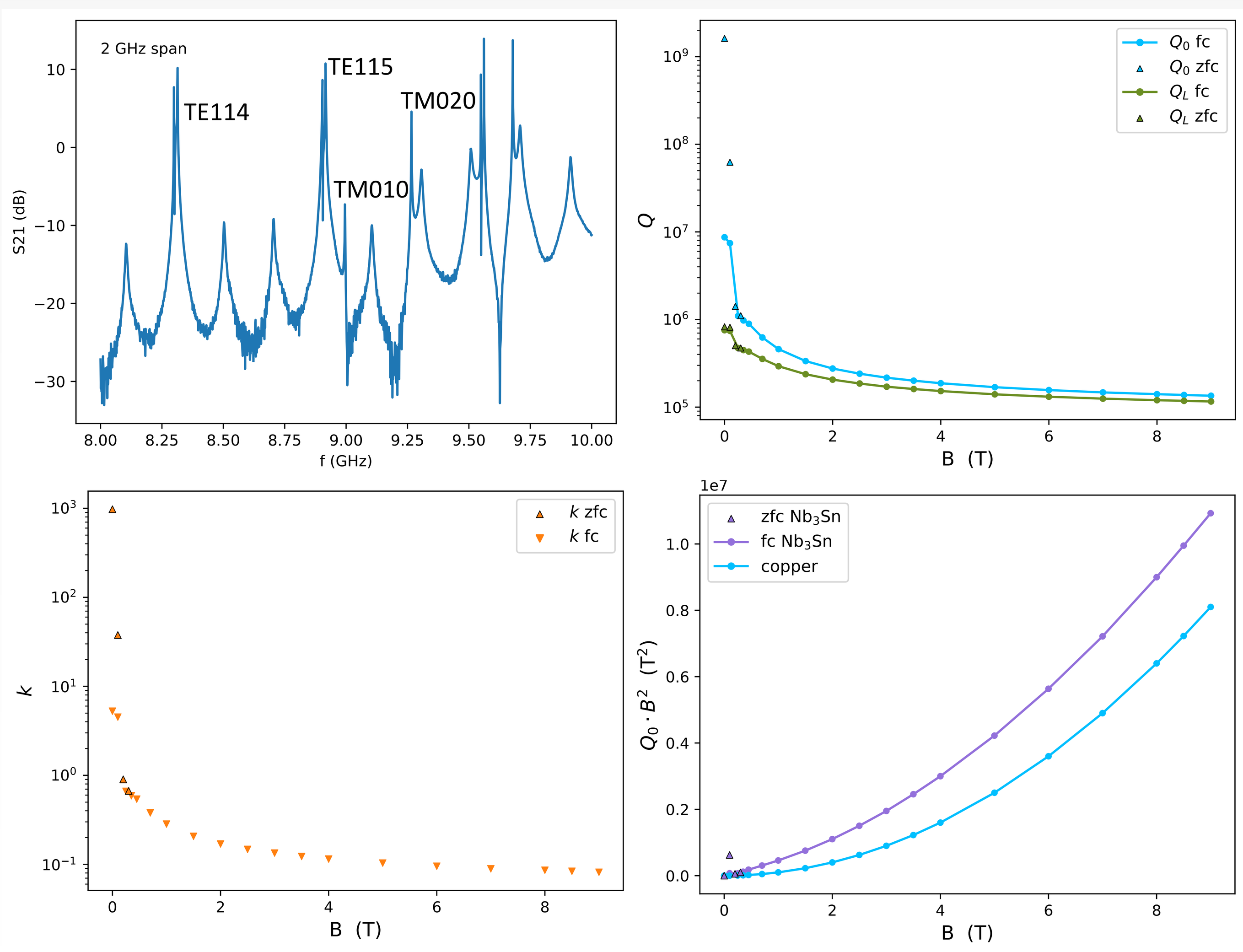

The cavity was characterized in the dilution refrigerator at LNF measuring its transmittivity S_{21} with a Vector Network Analyzer (VNA). The output rf line is amplified with a cryogenic HEMT at 4 K and a FET at room temperature, and the cavity is isolated with circulators. The magnet can provide a magnetic field ramping from 0 T to 9 T. After identifying the resonant modes, a measurement of the quality factor is performed. The VNA measures a loaded quality factor $Q_L = Q_0/(1+\kappa_1+\kappa_2)$, where $\kappa_{1,2}$ are the couplings of the injecting and reading antennas. To evaluate the Q_0, the couplings must be known, and the expression of the S_{21} can be used:

$$S_{21} = A \cdot \frac{2\sqrt{\kappa_1\kappa_2}}{1+\kappa_1+\kappa_2+jQ_0\delta} \simeq A \cdot \frac{2\kappa}{1+2\kappa+jQ_0\delta}$$

where A is the attenuation/gain of the input+output lines. In the hypothesis that $\kappa_1 = \kappa_2 = \kappa$ and that at 0 T the coupling κ is high, at resonance the expression becomes $S_{21} \simeq A$ and the attenuation can be estimated. Then, this is rescaled at higher B fields to obtain κ from direct S_{21} measurements. The results (orange plot) confirm that κ was large at 0 T and then decreases. The upper right plot shows the result of the extracted Q_0: it behaves as the simulated one, but its maximum value at 0 T is $\mathbf{1.6 \times 10^9}$, while at 9 T the value is $\mathbf{1.35 \times 10^5}$. This discrepancy could be due to a non-optimal mounting of the cavity, which has a small angle with respect to the magnetic field axis. The bottom right plot also shows the quantity $Q_0 B^2$, giving an idea of the improvement in sensitivity wrt classical copper cavities often used in axion searches. A factor ~ 2 could also be recovered aligning properly the cavity in the magnetic field.

Since the setup was the same as an actual axion search, we also performed a small data-taking of 1.5 h at 9 T. This was to verify that all the setup is working properly, confirming that the magnet can be permanently operated at maximum field. The data acquisition is performed by storing with an ADC the I and Q components of the downconverted signal, and then Fourier transforming them. The plot shows the extracted coupling constant $g_{a\gamma\gamma}$ of axions to photons, extracted by an analysis to the residuals of the cavity power spectrum. The parameters used for the analysis are reported in the table, and the result is about a factor of 10 from the benchmark model of KSVZ axions.

Together with the research on SC high-Q resonant cavities, the sensitivity for the axion discovery can be boosted with **quantum technologies**: as an example, the noise temperature is reduced from the current 5 K down to 0.5 K if a JPA is exploted; or the Standard Quantum Limit can be overcome if microwave single-photon counters based on JJs or qubits are developed in the next future.

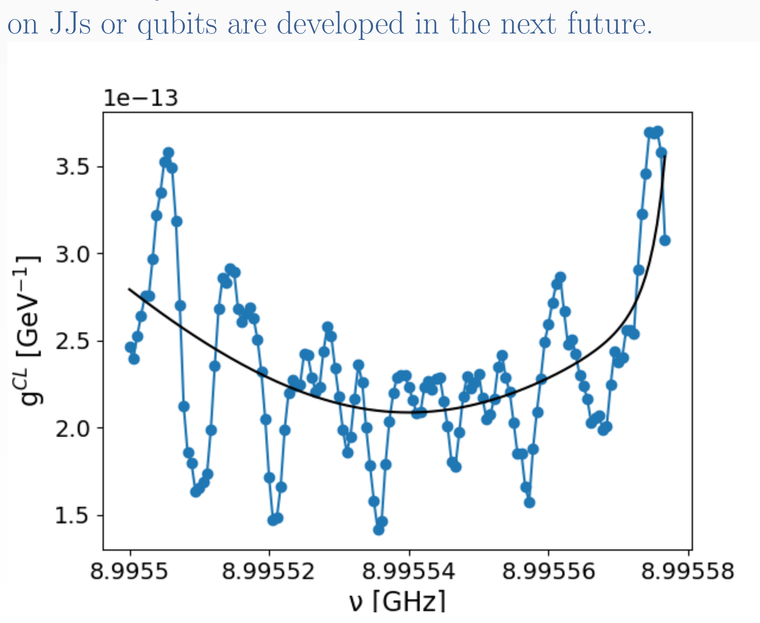

B_{av}	8.447 T
V_{cav}	0.068 L
C_{010}	0,69
β	0.08
Q_0	135000
freq	8.99554 GHz
Tcav	130 mK

Authors: A. Rettaroli, A. D'Elia, D. Di Gioacchino, C. Gatti, S. Lauciani, C. Ligi, G. Maccarrone, S. Tocci (from INFN–LNF); S. Posen, M. Checchin (from Fermilab–FNAL)

Erice, EMFCSC — 1–7 September 2023